THE OBSERVED GENERATION AND BREAKING OF ATMOSPHERIC INTERNAL GRAVITY WAVES OVER THE OCEAN*

S. SETHURAMAN

Department of Applied Science, Meteorology Group, Brookhaven National Laboratory, Upton, New York, U.S.A.

(Received 26 January, 1977)

Abstract. Observations are presented for internal gravity waves and their breaking at a height of 23.5 m over the ocean in surface-based inversions which are formed because of the advection of warm air over cold water. The spectral and cospectral analyses of velocity and temperature fluctuations were made to establish the characteristic features of the waves. Flow visualization photographs of smoke released during the breaking of a wave are also presented. Comparison between the turbulent energies present during and after breaking of a wave indicates enormous mixing and dispersion occurring during breaking.

1. Introduction

During stable atmospheric conditions, waves and turbulence co-exist and there is a non-linear interaction between them, the energy being fed from one to another. Identification of waves in flows where turbulence is small is probably not very difficult due to weakly ordered motion of waves as compared to random fluctuations of turbulence. In the atmospheric surface layer where the mechanical turbulence caused by the earth's surface is large, identification of waves would be somewhat difficult. Here again, the relative magnitude of waves and turbulence becomes important in the analysis. Philips (1960) and Bretherton (1969) amongst others have advanced theoretical approximations to model internal gravity waves. Several studies of internal gravity waves (Axford, 1970, 1971, for example) have been at very high altitudes, carried out to understand the contribution of the waves to clear-air turbulence. Metcalf and Atlas (1973) and Metcalf (1975) using aircraft-mounted instruments, studied waves at low-level inversions with the base of the inversions a few hundred meters above the surface. Caughey and Readings (1975) described waves within 183 m above the earth's surface during nocturnal inversions over land.

This paper describes observations of internal gravity waves very near the surface (within a height of 24 m) in the surface-based inversion of the marine boundary layer. Several conflicting features that would probably affect the generation of internal gravity waves in the marine surface layer are: (1) Nearness of the boundary – increases turbulence, (2) Smooth surface – decreases turbulence, (3) Large body of water – minimal diurnal variation in surface temperature, (4) Wind-generated surface waves – contributes to atmospheric turbulence at certain frequencies. The

* This research was performed under Contract No. EY-76-C-02-0016 with the United States Energy Research and Development Administration.

Boundary-Layer Meteorology **12** (1977) 331–349.

internal gravity waves discussed here occurred in the surface-based advective inversions in contrast to observations of waves in the subsidence and nocturnal inversions reported in the literature. The data were obtained on June 19, 1975 as part of the coastal meteorological studies conducted by Brookhaven National Laboratory (Raynor *et al.*, 1975).

2. Measurements

Mean wind speeds were observed at 3.35, 7, 10.7, 14.3, 16.2 and 23.5 m on a 24-m tower located close to the beach; standard 3-cup anemometers were used. Longitudinal, lateral and vertical velocity fluctuations were measured at a height of 23.5 m with a Vector Vane whose frequency response was in excess of 1 Hz (a distance constant of about 0.6 m) for moderate wind speeds (SethuRaman and Brown, 1976). In addition, temperature fluctuations were measured by thermistors at 3.35, 10.7, 18 and 23.5 m. The thermistors had a time constant of about 4 s at a wind speed of about 5 m s^{-1}. Mean relative humidity was measured at different heights on the 24-m tower, using a portable humidity sensor every 30 min. The tower is located about 30 m from the ocean. Mean temperatures over water to a height of 900 m were measured with an aircraft-mounted thermistor. Pilot-balloon soundings were made at the beach to obtain wind speeds and directions at higher elevations.

3. Data

The synoptic situation that existed on June 19, 1975 at 0700 EST is shown in Figure 1. A weak high pressure area was located over Virginia causing west to southwesterly winds at the experimental site on the south shore of Long Island. With the air flowing at a shallow angle to the beach (less than 45 deg), over-water fetch is usually a few hundred kilometers. This fetch is sufficient to form a strong surface-based inversion of a few hundred meters thick but not enough for the air mass to adjust to surface temperature conditions completely (SethuRaman, 1976). The mean potential temperature profile shown in Figure 2 indicates a 300-m deep surface-based inversion with steepest temperature gradients near the surface. For internal waves, the restoring force is characterized by the Brunt–Väisälä frequency

$$N = \left\{ \frac{g}{\bar{\theta}} \frac{\mathrm{d}\theta}{\mathrm{d}z} \right\}^{1/2} \tag{1}$$

where g is the gravitational acceleration, $\bar{\theta}$ the mean absolute potential temperature and $\mathrm{d}\theta/\mathrm{d}z$ the potential temperature gradient. Referring to Figure 2, there seem to be three regions of differing temperature gradients, viz., 0–50, 50–150 and 150–300 m. But due to lack of observations between 24 and 150 m, the entire height of 300 m is considered to be a single slab for the computation of N, yielding a value of 0.033. Mean temperature measured an hour later indicated slight warming, but the temperature structure was essentially reproduced.

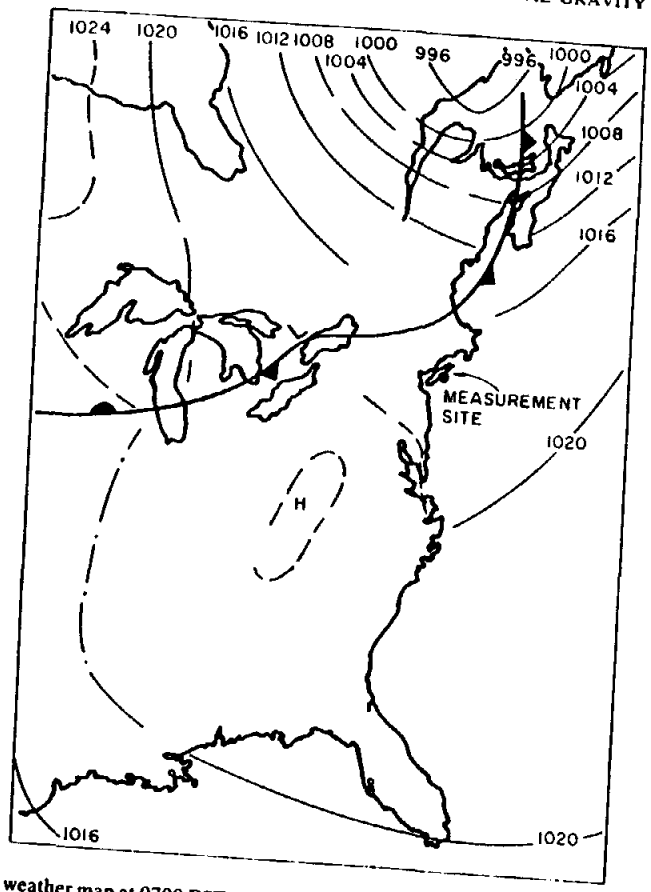

Fig. 1. Surface weather map at 0700 EST, June 19, 1975 showing the synoptic conditions in the vicinity of the measurement site.

Wind speeds and directions obtained by pilot-balloon observations are shown in Figure 3 along with the mean of the two successive observations. Substantial acceleration of wind and directional shear within the inversion, similar to a nocturnal jet, is present. Figure 4 shows the fluctuations of vector wind speed, elevation angle and horizontal angle at 23.5 m related to longitudinal (along the mean wind direction), lateral and vertical wind speeds for a period of 55 min, in which well-defined waves are seen with turbulence superimposed. The linear regression line is nearly horizontal indicating no trend for this time period. Towards the right of Fig. 4, corresponding to the time period 45–55 min, the beginning of a burst phenomenon is apparent. Simultaneous temperature fluctuations measured at 3.35, 10.7, 18 and 23.5 m are shown in Figure 5. The mean temperatures also indicate well-defined waves for this time period with the same periodicity as the wind. As the height of

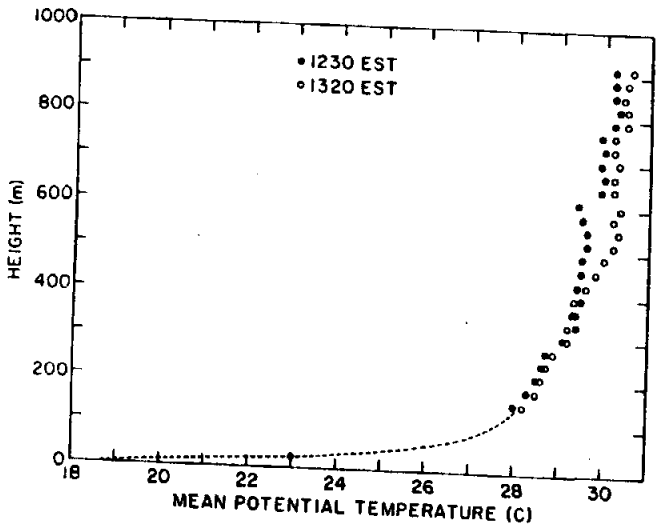

Fig. 2. Mean potential temperature profile measured by the aircraft 2 km offshore. Interpolation between the aircraft values, the tower temperature and surface temperature of water is shown dotted.

observation decreased, turbulence became more pronounced. The internal boundary layer developing at the land–sea interface was about 10 m thick. Waves of significant amplitudes were observed even within the internal boundary layer (see Figure 5) where the mean temperatures were in the process of changing to superadiabatic lapse rate. This could probably happen only in the transition zone where the boundary layer was still developing. The turbulence data were digitized at 0.5-s intervals and a conventional spectral analysis carried out (Blackman and Tukey, 1958).

4. Analysis

A flow is usually called turbulent if it has random vorticity distribution and is highly diffusive compared to molecular diffusivities (Busch, 1969; Stewart, 1969). Also in a turbulent flow, energy will be transferred from one scale to another through a continuous cascade process. On the other hand, wave motion lacks diffusive character and propagates through the medium with respect to a coordinate system moving with a velocity specified by the mean flow. When the waves co-exist with turbulence in the atmospheric surface layer, spectral and co-spectral analysis seems to be one of the powerful tools to detect waves and their harmonics. This procedure has been used by Axford (1971), Metcalf and Atlas (1973), Caughey and Readings (1975) and Metcalf (1975) among others. In the following sections, analysis of the data in the frequency domain is carried out to establish the presence of the waves and to determine the characteristic features. The observations were pre-averaged to have a sampling time of 10 s. This permitted reliable spectral density computations at low

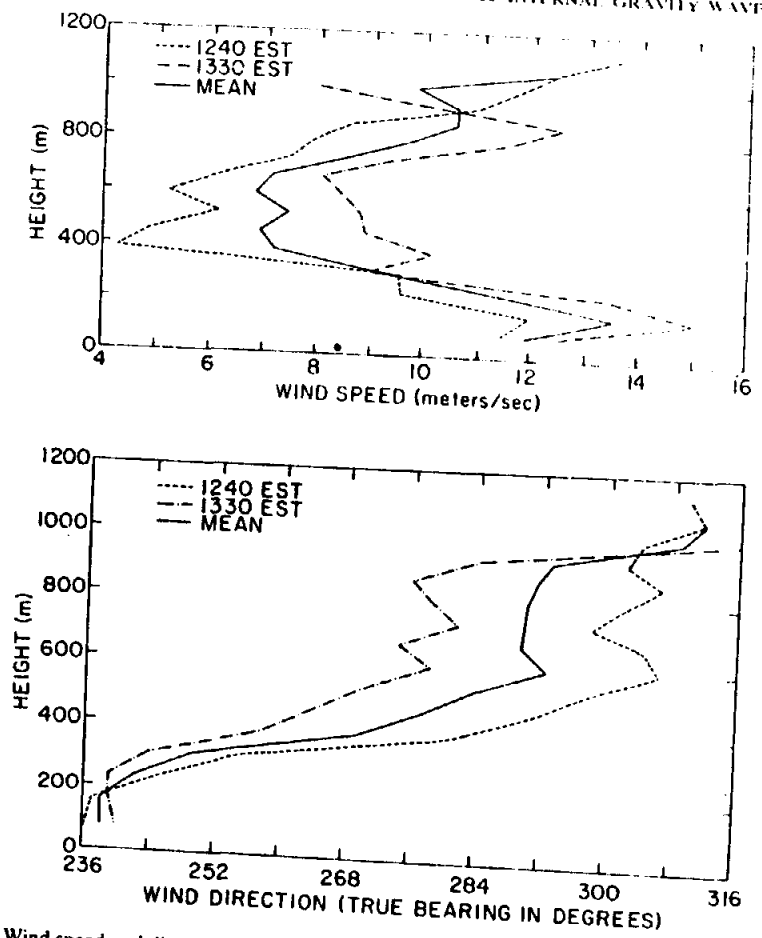

Fig. 3. Wind speed and direction up to a height of 1000 m obtained by pilot-balloon soundings at the beach. Solid circle represents the mean wind speed measured at 23.5 m.

frequencies and provided meaningful analysis for temperature measurements made by the relatively low-response thermistors. Spectral analysis of turbulence data was also carried out without any pre-averaging to study the higher frequencies.

4.1. Autocorrelation functions

The auto covariance $\alpha(t_1)\alpha(t_2)$ where α is the variable under consideration is a function only of the time difference $t_2 - t_1$ for a stationary process and is sometimes normalized by dividing by the variance to obtain an autocorrelation function $R(t)$ given by

$$R_\alpha(t) = \frac{\overline{\alpha(t)_1 \alpha(t)_2}}{\overline{\alpha^2}}. \qquad (2)$$

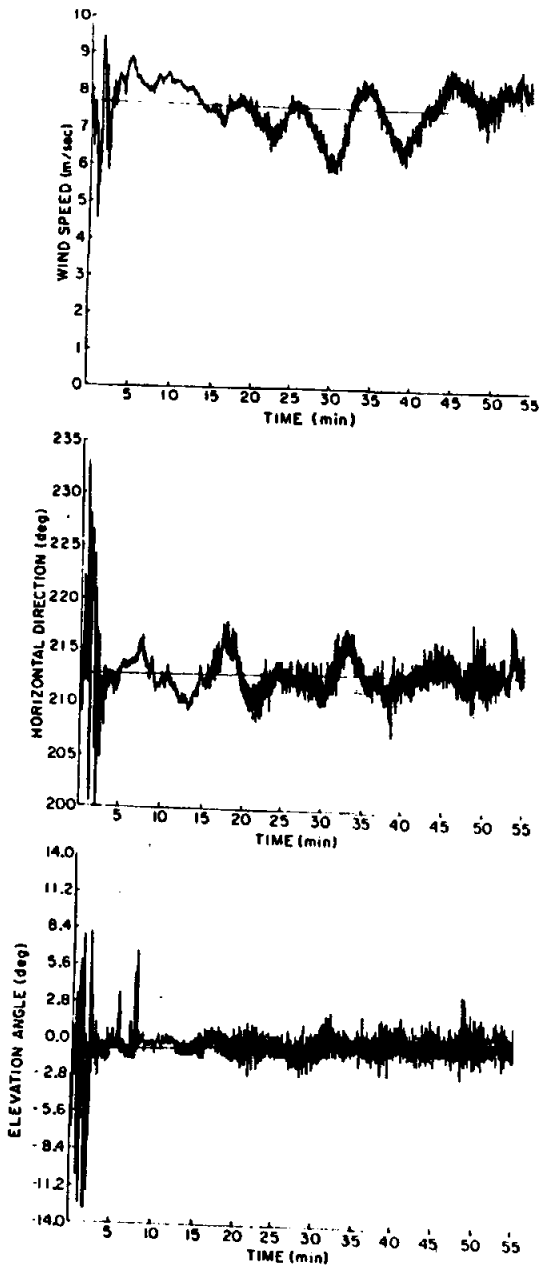

Fig. 4. Time history of vector wind speed, horizontal angle, and vertical angle fluctuations at 23.5 m. Solid line through the data is a linear regression line. Starting time was 1235 EST.

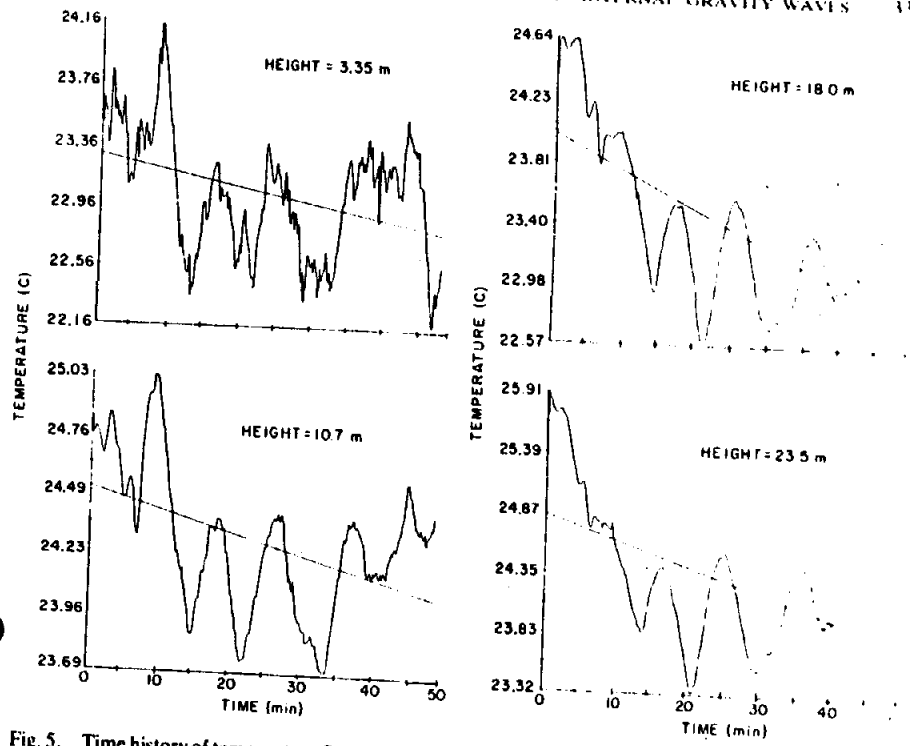

Fig. 5. Time history of temperature fluctuations at 3.35, 10.7, 18, and 23.5 m. Solid line through the data is a linear regression line. Starting time was 1245 EST.

The correlogram of a sinusoidal time series with period P is a cosine curve having the same period and an amplitude of unity. On the contrary, a typical correlogram of atmospheric turbulence drops off rapidly and oscillates around zero for large time lags. Hence, an autocovariance analysis was made to determine its features for a combination of waves and turbulence. Figure 6 shows the autocorrelograms for R_u, R_v, R_w and R_0. The observations were made at 23.5 m above the surface.

Several important deductions can be made by comparing the different autocorrelation functions. All of them have the maximum positive covariance around a lag period of about 500 s although each one of them has its own distinct features. None of them has symmetrical shape; but R_u seems to have the largest positive and negative values of covariance. R_v and R_w have approximately the same normalized covariance value at the first harmonics with the peaks occurring at slightly different time lags. The reason for very small negative covariances (close to zero) for R_v and R_w is not readily apparent although the effect of the turbulence caused by mechanical roughness and breaking waves of different harmonics cannot be ruled out.

4.2. Spectra

The spectral density S is defined as the Fourier transform of the correlation function

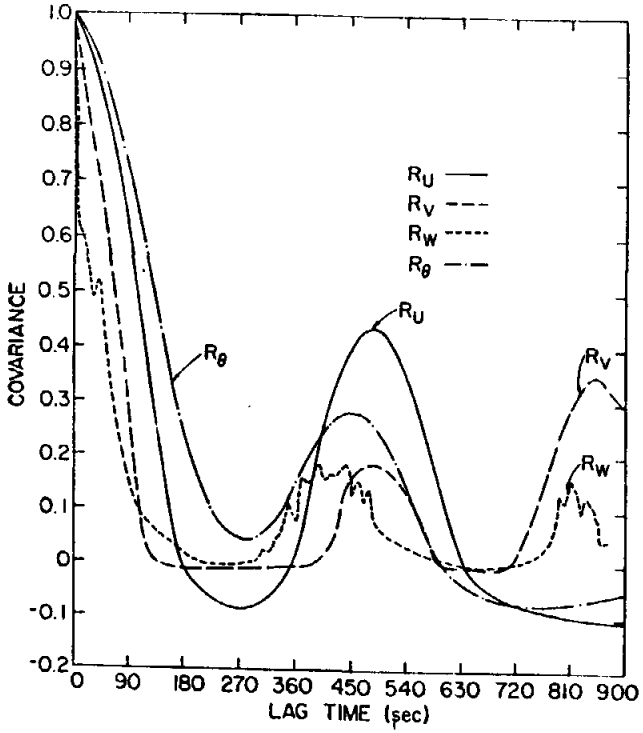

Fig. 6. Autocorrelograms of u, v, w, and θ using data recorded between 1245 and 1330 EST.

of the velocity fluctuations and has a property that

$$\overline{\alpha^2} = \int_0^\infty S_\alpha(n)\,dn = \int_0^\infty S_\alpha(k)\,dk \qquad (3)$$

where α is the variable under consideration, n is the cyclic frequency, k is the wave number as $2\pi n/\bar{u}$, and $S(k)$ is the one-dimensional energy spectrum whose subscript indicates the variance or covariance to which it contributes. Individual spectra for a period of about 50 min when wave action was dominant for longitudinal (u), lateral (v), and vertical (w) velocity fluctuations are shown in Figure 7. When a wave is present, the spectra should indicate peaks associated with high levels of coherence. the spectra shown in Figure 7 have well-defined peaks around a frequency of 0.002 Hz. The wavy pattern of the spectra involving the harmonics of this frequency and the steep slopes approximating n^{-4} behind the peaks are also characteristic of the presence of an equilibrium field of breaking waves. The data were pre-averaged to 10 s for the above analysis in order to extend the spectra to sufficiently low frequencies for wave action to be dominant. Analysis of the high frequency part of the spectrum obtained without any pre-averaging also indicated similar features as shown in Figure 8, but the general slope of v and w spectra began to approximate

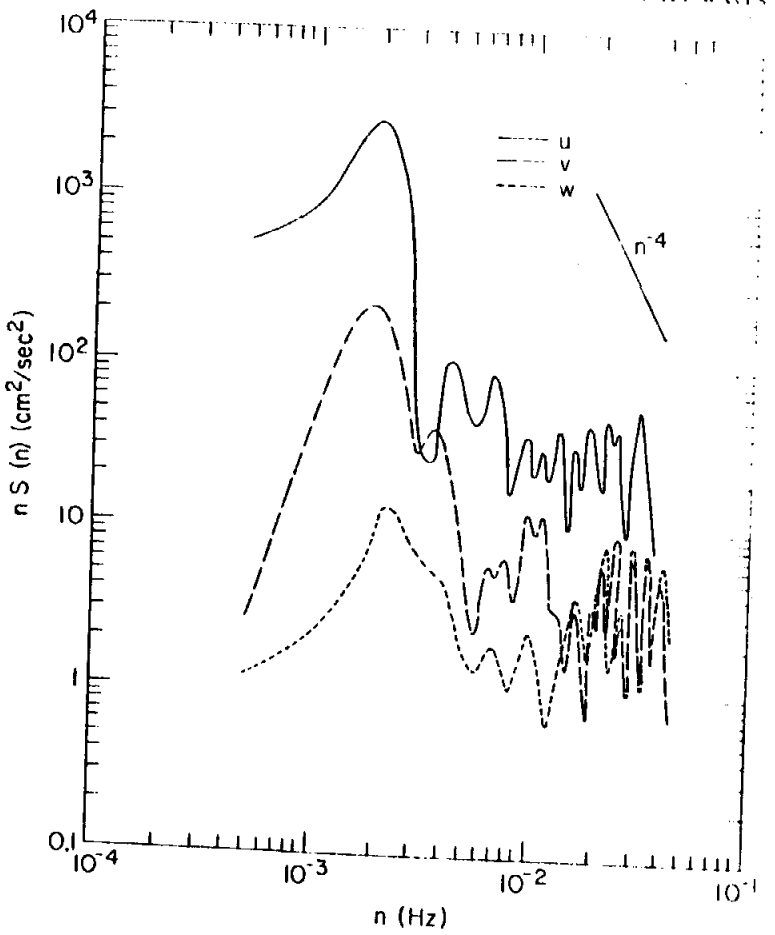

Fig. 7. Low-frequency spectra of u, v, and w. The data between 1245 and 1330 EST were pre-averaged to 10 s before analysis.

$n^{-2/3}$. The spectral densities of v and w components were also higher than that of u component, one of the requirements for the onset of the inertial subrange. In turbulent flows, the inertial subrange usually begins at frequencies as low as 0.5 for a height of 24 m. The cascading process characteristic of turbulent flows is shifted to higher frequencies when waves are present.

4.3. Cross-spectra

The cross-spectra $\overline{uw}$, $\overline{vw}$, and $\overline{uv}$ are shown in Figure 9 and the cross-spectra $\overline{u\theta}$ and $\overline{w\theta}$ in Figure 10. All the cross-spectra show the anticipated peaks near frequency of 0.002 Hz associated with the waves. The phase angle $\phi_{\alpha\beta}(n) = \tan^{-1}[Q_{\alpha\beta}(n)/Co_{\alpha\beta}(n)]$, where α and β are the two variables considered, $Co_{\alpha\beta}(n)$

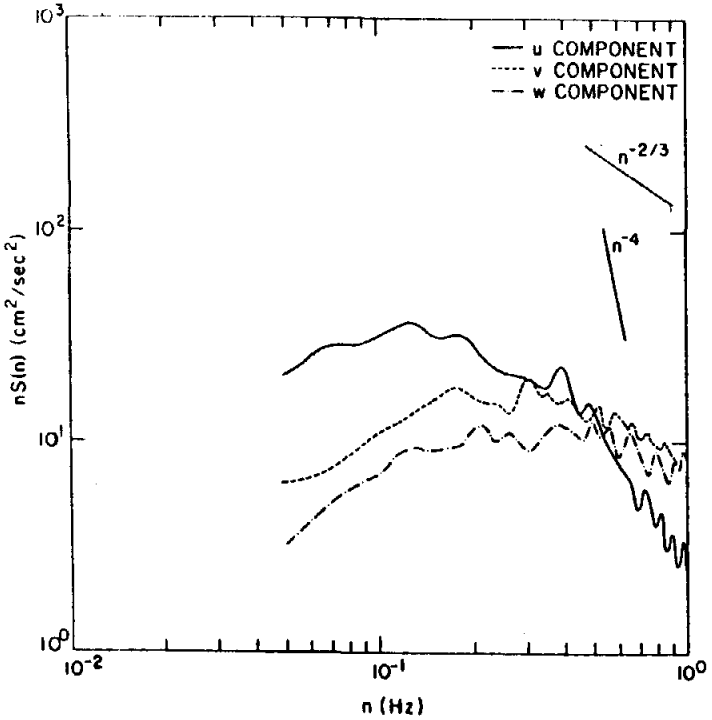

Fig. 8. Higher frequency spectra of u, v, and w for the data between 1300 and 1330 EST. The sampling time was 0.5 s.

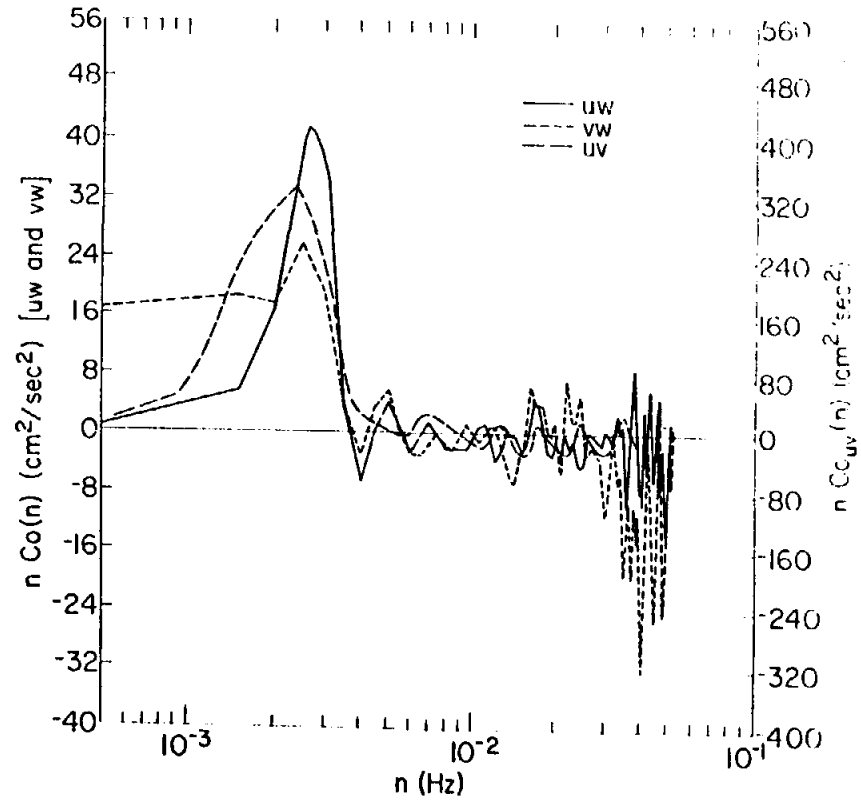

Fig. 9. Cross-spectra $\overline{uw}$, $\overline{vw}$, and $\overline{uv}$ for the individual spectra corresponding to Figure 7.

the Cospectra and $Q_{\alpha\beta}(n)$ is the Quadrature spectra, represents the average phase difference between common frequency components of the two variables. The coherence given by $[Co^2_{\alpha,\beta}(n)+Q^2_{\alpha,\beta}(n)]/S_\alpha(n)S_\beta(n)$ yields a measure of the correlation between the two variables as a function of frequency.

The coherence and phase angle for the dominant frequency of $0.002 < n < 0.003$ is given in Table I. In wave motion, the vertical velocity fluctuations w and temperature fluctuations θ should be about 90 deg out of phase. In turbulence, the phase lag is generally much smaller. The phase angle for $\overline{w\theta}$ was 99°, for $\overline{uw}$, −81° and for $\overline{u\theta}$, 15°. These are consistent with the values expected from theoretical considerations. Values given by Axford (1971) for gravity waves in the lower stratosphere are in agreement with the above results. Caughey and Readings (1975) found values of $\overline{w\theta}$, $\overline{u\theta}$ and $\overline{uw}$ to be 48, 72 and 22°, respectively, in their study of internal waves in nocturnal inversions at a height of 183 m. They concluded that phase relationships cannot be used to identify waves near the earth's surface due to the co-existence of turbulence. The present study indicates that the theoretical phase relationships are valid even at a height of about 24 m for a stable atmospheric flow. If the peaks are interpreted as a group of waves, then the six values of ϕ are not independent; or for example, if θ is considered to be the first wave variable, then the last three columns define u to lag w by 84°, u to lag v by 47° and v to lag w by 37°. Comparing these values with those in the first 3 columns of Table I, it can be seen that the analysis has produced results compatible within 3°. The coherences ranged from 0.62 to 0.96 as shown in Table I. Cross-spectral computations between the temperature fluctuations at different levels indicated high coherences (in excess of 0.9) for 18 and 23.5 m. As the vertical separation distance increased, the coherence decreased appreciably.

4.4. Cascade process

Another diagnostic tool helpful in distinguishing internal waves from turbulence is a quantity q representative of the number of cycles it takes to change the kinetic energy of the motion E by an amount comparable with E (Busch, 1969). q is given by

$$q = fE/(\partial E/\partial t)$$

where f is a characteristic frequency associated with a given motion (taken to be

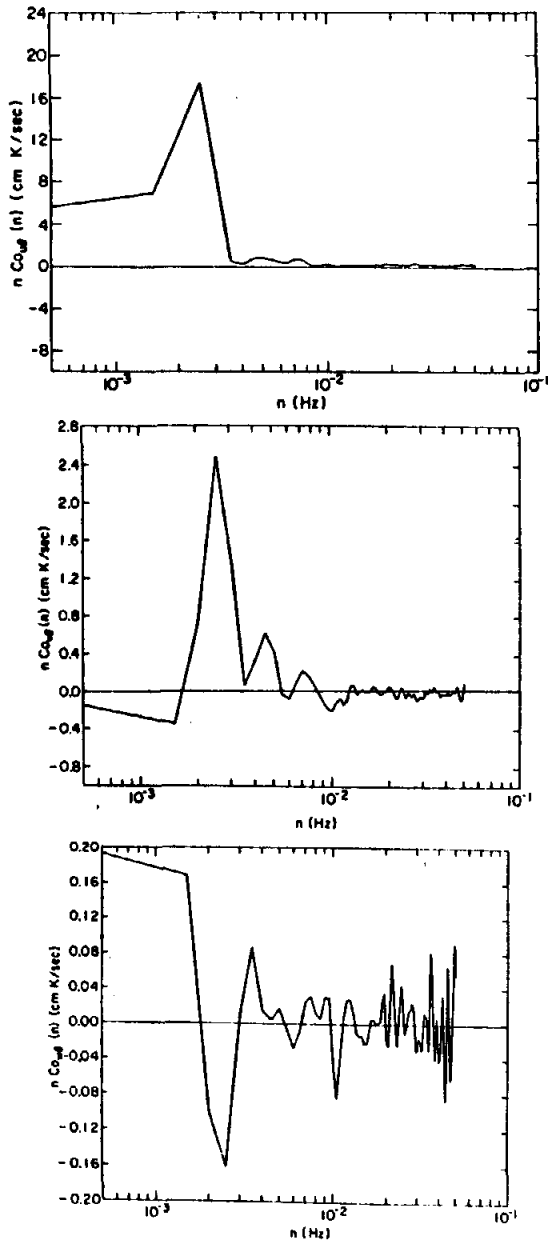

Fig. 10. Cross-spectra $\overline{u\theta}$, $\overline{v\theta}$, and $\overline{w\theta}$.

TABLE I

Phase angles and coherence for $0.002 < n < 0.003$

	$\overline{uv}$	$\overline{uw}$	$\overline{vw}$	$\overline{u\theta}$	$\overline{v\theta}$	$\overline{w\theta}$
ϕ in deg.	−45	−81	−34	15	62	94
Coherence	0.62	0.81	0.78	0.96	0.75	0

$E^{1/2}/l$ where l is the space scale, when a better estimation of this frequency is available) and $\partial E/\partial t$ is the rate of spectral energy transfer obtainable from inertial subrange. For a turbulent field, q is close to 1. To compute q, the characteristic frequency was assumed as the Brunt–Väisälä frequency equal to 0.033 Hz. $\partial E/\partial t$ was estimated from the inertial subrange of the v spectra as 0.44 cm^2 s^{-3}. With the total kinetic energy, $E = \sigma_u^2 + \sigma_v^2 + \sigma_w^2 = 1849$ cm^2 s^{-2}, q was found to be which is far in excess of 1.

4.5. Characteristics of the Wave

Some insight into the structure of the wave may be obtained by considering a simple two-dimensional wave equation of the form (Caughey and Readings, 1975),

$$Z = a \sin(kx - \omega t)$$

where Z is the vertical displacement, k the wave number, ω the intrinsic frequency of the wave in rad s^{-1} (i.e., the frequency relative to the air in which the wave occurs), x is the horizontal position and t is the time. Vertical oscillations of the wave are given by

$$W = \frac{dZ}{dt} = -(a\omega)\cos(kx - \omega t).$$

The velocity of the wave relative to air at height z is

$$C(z) = \omega/k$$

and the observed time period of the wave τ_0 is given by

$$\tau_0 = \frac{\lambda}{U(z) + C(z)}$$

where λ is the wavelength and $U(z)$ the mean wind speed. This assumes that the wave is propagating in the direction of the wind. The intrinsic frequency n_w of the wave can be deduced from the amplitude of the oscillations of vertical velocity from Equation 6 as

$$a_w = a\omega = 2\pi a n_w.$$

From the considerations of the variation of potential temperature with height and mean temperature perturbations, the amplitude of the wave, a, was estimated from

10 m. The amplitude of the vertical velocity oscillations was about 0.06 m s^{-1} yielding an intrinsic frequency of 0.0009 Hz.

Adopting the method used by Hooke *et al.* (1973), n_w is related to the local Brunt–Väisälä frequency by

$$\left\{\frac{N^2}{n_w^2}-1\right\}^{1/2}=\frac{\Delta U}{\Delta W} \tag{10}$$

where ΔU and ΔW are the amplitudes of the horizontal and vertical velocity perturbations, respectively. From the data, $\Delta U/\Delta W \simeq 36$ and $N=0.033$. Using Equation (10), $n_w = 0.00092$ Hz which is very close to the value obtained from the amplitudes of the vertical velocity oscillations. Rewriting Equation (8) with $n_0 = 1/\tau_0$ and $C(z) = \lambda n_w$,

$$\lambda = \frac{U(z)}{n_0 - n}. \tag{11}$$

With $n_0 = 0.0024$ estimated from Figure 4 and with a wind speed of 6.4 m s^{-1}, the wavelength $\lambda = 4.3$ km and $C(23.5) = 3.8$ m s^{-1}. For a wave height of about 10 m, he wavelength seems to be reasonable although three-dimensionality of the wave itself should be taken into account to obtain more correct values.

In fact, if θ is the angle to the horizontal at which the wave propagates, it is given by the relationship

$$\theta = \cos^{-1}(n_w/N). \tag{12}$$

For the values of n_w and N estimated here, θ is close to 88 deg indicating the possibility of a vertically propagating wave. Since the quantity uw was positive during he period of wave propagation and hence the Reynolds Stress negative, it can be shown that the internal wave was propagating downward and the energy extracted from the wave motion was transferred to the mean flow (Phillips, 1966). Using the angle determined from Equation (12), the wavelength in a horizontal plane can be computed to be about 120 m, which is close to the values inferred from photographs.

5. Breaking Phenomenon

Breaking of internal waves seems to be a problem not very well understood. For waves of different modes, overturning may occur due to the distortion of one mode in the velocity field of another (Davis and Acrivos, 1967). For a single wave mode, unstable density gradients may occur where the local horizontal particle speed xceeds the phase speed of the wave (Orlanski and Bryan, 1969) when the amplitude f a wave exceeds a critical amplitude. These unstable gradients contribute towards a nvective instability in a small volume of fluid. Such breakdown is not complete and e waves may reform. Some unique flow visualization photographs taken during and fter a typical internal wave breaking in the course of the experiment will be

presented in this section. A comparison will also be made between various par ters, during and after breaking to understand the degree of interaction.

Although detailed study of the atmospheric variables at the tower is for only hours on days when the required meteorological conditions were met, the wind s and direction measured by an aerovane were recorded continuously. Figur shows the direction trace for a period of about 90 min starting at 1210 EST exten over the period in Figure 4 during which detailed observations were made. Refe to Figure 11, two significant bursts can be seen; one at 1220 for 5 min and anoth 1235 for 3 min. The second burst of turbulence corresponding to the first 3 m Figure 4 is the subject of analysis in the following paragraphs. Mean wind sp turbulent fluxes and energies for a period of 15 min beginning at 1235 E.S intervals of 3 min are given in Table II. The first interval corresponds to the bur turbulence shown in Figure 4 due to the breaking of internal waves. This is follo by a period when a group of internal gravity waves was observed at the t Certain interesting features are apparent from the Table. As expected, turbu fluctuations were significant during breaking, variance being several times hi than the corresponding values when the breaking phenomenon was absent. I downward fluxes of momentum in the streamwise direction were present durin breaking process yielding a friction velocity u_* in excess of 30 cm s^{-1}. During ne conditions or slightly stable conditions when internal gravity waves are absen

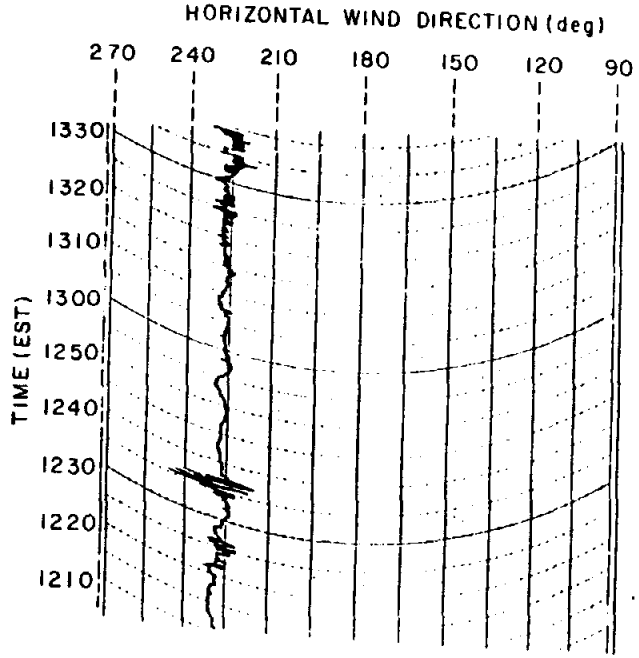

Fig. 11. Wind direction for the period before and during the experiment, showing the bursts of turbu

TABLE II

Mean and turbulent parameters at different stages of internal gravity waves

Starting time	Time interval (min)	$\bar{u}$	σ_u	σ_v (cm s^{-1})	σ_w	$\overline{uw}$	$\overline{vw}$	$\overline{uv}$ (cm s^{-1})^2	Turbulent Energy
1135	3	714	105	81	54	−1106	517	264	10251
1138	3	817	35	18	9	−2	−9	66	815
1141	3	836	28	7	9	−19	0	20	457
1144	3	829	11	11	4	−2	5	−45	129
1147	3	787	21	8	5	−3	8	−27	265

hardly exceeds 20 cm s^{-1} over water. Downward momentum flux decreased to near zero when breaking did not occur, indicating the dominance of wave action over turbulence in transporting momentum. Turbulent energy was found to be about 100 times higher during breaking. Some of this significant energy is obviously fed back into the mean flow and the internal waves in a non-linear fashion. As can be seen from Table II, the mean wind speed increased by about 15% in the next five minutes before leveling off.

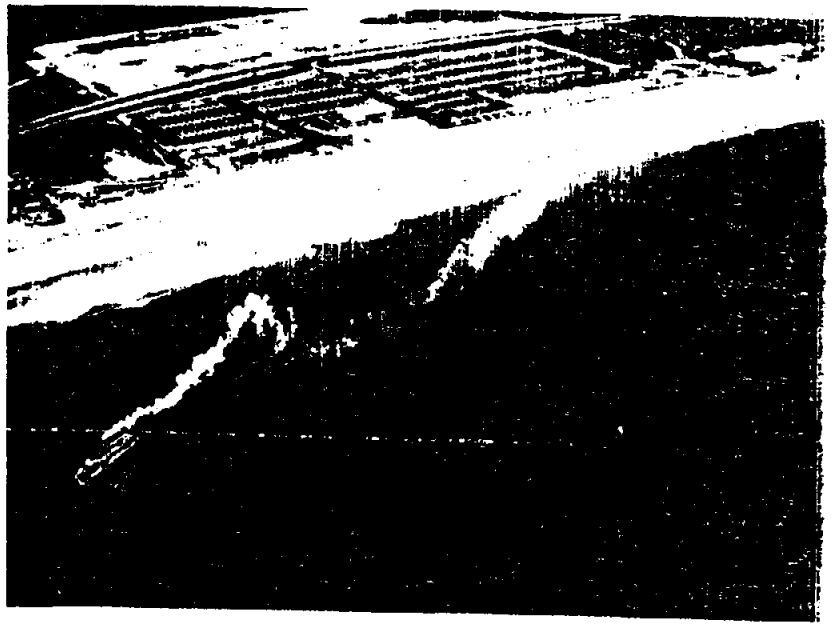

Fig. 13. Photograph of the smoke during the breaking of the waves (time 1237 EST) from the aircraft.

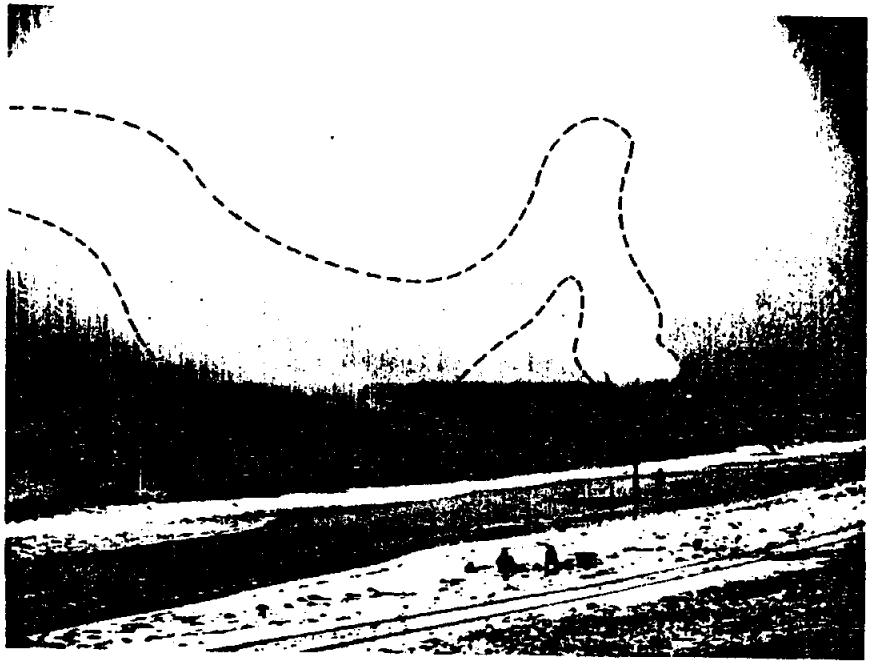

Fig. 12. Photograph of the smoke during the breaking of the waves (time 1237 EST) taken from the beach.

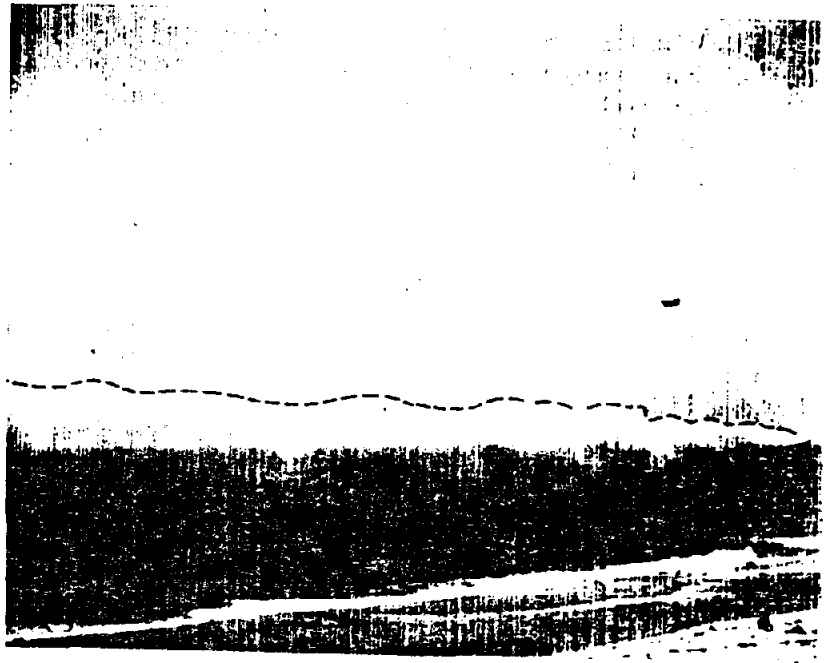

Fig. 14. Photograph of the smoke when there was no wave breaking (time 1240 EST) from the beach.

While the internal waves were in the process of breaking, some flow visualization photographs were taken of the oil-fog smoke released over water, from the beach and also from an aircraft. The smoke was released from a boat at a height of about 8 m above the water surface and about 400 m offshore. Figure 12 is an elevation view of the smoke during the breaking of internal waves showing the tremendous looping and dispersion. The degree of dispersion in Figure 12 would be hard to believe and comprehend if it were not for the values presented in Table II. Figure 13 is the plan view of the smoke photographed from a low-flying aircraft showing the lateral dispersion present during breaking. This is not totally surprising if we compare it to the time history of wind direction in Figure 4. A photograph showing the elevation view of the smoke released from the boat at the same position at 1240 EST (two minutes after breaking) is shown in Figure 14. The strong dispersion seen in Figure 12 is absent and the smoke is more coherent.

6. Conclusions

Internal gravity waves have been shown to exist over water near the surface in a surface-based inversion formed due to the advection of warm air over cold water. When turbulence and waves co-exist near the surface, spectral and cross-spectral analysis, which yields dominant peaks, coherence and phase angle relationships, seems to be a valuable tool in identifying and characterizing waves. Breaking of waves produces large amounts of momentum flux and turbulent energy, some of which is fed back into the wave system. Wavelength, amplitude and velocity of the wave obtained from a simple two-dimensional model seems to be of comparable magnitude to those in other studies (Gossard *et al.*, 1970). Propagation of gravity waves and their breaking involve a wide range of atmospheric scales. These waves are important geophysical phenomena to be aware of when conditions are conducive for their generation.

Acknowledgements

G. S. Raynor and R. M. Brown took part in planning and directing the experiment reported here. J. McNeil, A. Tuthill, W. Jahnig and J. Tichler assisted in various aspects of data acquisition and analysis. The author appreciates several helpful discussions with R. T. Cederwall. Research was performed under the auspices of the U. S. Energy and Development Administration.

References

Axford, D. N.: 1970, 'An Observation of Gravity Waves in Shear Flow in the Lower Stratosphere', *Quart. J. Roy. Meteorol. Soc.* **96**, 273–286.

Axford, D. N.: 1971, 'Spectral analysis of an Aircraft Observation of Gravity Waves', *Quart. J. Roy. Meteorol. Soc.* **97**, 313–321.

Blackman, R. B. and Tukey, J. W.: 1958, *The Measurement of Power Spectra*, Dover Publications, N York.

Bretherton, F. P.: 1969, 'Waves and Turbulence in Stratified Fluids', *Radio Science*, **4**, 1279–1287

Busch, N. E.: 1969, 'Waves and Turbulence', *Radio Science*, **4**, 1377–1379.

Caughey, S. J. and Readings, C. J.: 1975, 'An Observation of Waves and Turbulence in the Ear Boundary Layer', *Boundary-Layer Meteorol.* **9**, 279–296.

Davis, R. E. and Acrivos, A.: 1967, 'The Stability of Oscillatory Internal Waves', *J. Fluid Mech* 723–736.

Gossard, E. E., Richter, J. H., and Atlas, D.: 1970, 'Internal Waves in the Atmosphere from H Resolution Radar Measurements', *J. Geophys. Res.* **75**, 3523–3536.

Hooke, W. H., Hall, F. F., and Gossard, E. E.: 1973, 'The Observed Generation of an Atmosph Gravity Wave by Shear Instability in the Mean Flow of the Planetary Boundary Layer', *Bound Layer Meteorol.* **5**, 29–41.

Metcalf, J. I.: 1975, 'Gravity Waves in a Low-Level Inversion', *J. Atmos. Sci.*, **32**, 351–361

Metcalf, J. I. and Atlas, D.: 1973, 'Microscale Ordered Motions and Atmospheric Structure Associ with Thin Echo Layers in Stably Stratified Zones', *Boundary-Layer Meteorol.* **4**, 7–35.

Orlanski, I. and Bryan, K.: 1969, 'Formation of the Thermocline Step Structure by Large-Amplitu Internal Gravity Waves', *J. Geophys. Res.* **74**, 6975–6983.

Phillips, O. M.: 1960, 'On the Dynamics of Unsteady Gravity Waves of Finite Amplitude. Part 1 Elementary Interactions', *J. Fluid Mech.* **9**, 193–217.

Phillips, O. M.: 1966, *The Dynamics of the Upper Ocean*, Cambridge University Press, England, 261 pp

Raynor, G. S., Michael, P., Brown, R. M., and SethuRaman, S.: 1975, 'Studies of Atmospheric Diffus from a Near Shore Oceanic Site', *J. Appl. Meteorol.*, **14**, 1080–1094.

SethuRaman, S.: 1976, 'Air Mass Modification Due to Change in Surface Characteristics', *Mon. Weat Rev.* **104**, 1040–1043.

SethuRaman, S. and Brown, R. M.: 1976, 'A Comparison of Turbulence Measurements Made b Hot-film Probe, a Bivane, and a Directional Vane in the Atmospheric Surface Layer', *J. Appl. Meteo* **15**, 138–144.

Stewart, R. W.: 1969, 'Turbulence and Waves in a Stratified Atmosphere', *Radio Science*, **4**, 1269–1278